

INFLUENCE OF STRESS TRANSFER IN PROBABILITY ESTIMATES OF $M \geq 6.5$ EARTHQUAKES IN GREECE AND SURROUNDING AREAS

**Paradisopoulou P. M.¹, Papadimitriou E. E.¹, Karakostas V. G.¹,
Lasocki S.², Mirek J.³, Kiliass A.⁴**

¹ *Geophysical Laboratory, School of Geology, Aristotle University of Thessaloniki, PO Box 352-1, 54006, Thessaloniki, ppara@geo.auth.gr, ritsa@geo.auth.gr, vkarak@geo.auth.gr*

² *Institute of Geophysics, Polish Academy of Sciences, Warsaw, Poland, lasocki@igf.edu.pl*

³ *Faculty of Geology, Geophysics and Environmental Protection, AGH University of Science and Technology, Krakow, Poland, jmirek@seismo.geol.agh.edu.pl*

⁴ *Department of Geology, School of Geology, Aristotle University of Thessaloniki, GR-54124, Thessaloniki, Greece, kiliass@geo.auth.gr*

Abstract

The coseismic stress changes due to strong earthquakes ($M \geq 6.5$) that occurred in Greece and its adjacent areas since the beginning of the 20th century (instrumental era) are calculated and the future seismic hazard expressed in terms of the probabilities of occurrence of $M \geq 6.5$ events is assessed. Calculations of the change in Coulomb failure stress reveal that 61 out of 67 ruptures were brought closer to failure by the preceding shocks. A new insight on the evaluation of future seismic hazards, in the study area, is given by translating the calculated coseismic stress changes into earthquake probability. We incorporated the effect of stress change into the time-dependent probability estimates using an earthquake nucleation constitutive relation, which includes both permanent and transient effects of stress changes. Taking into account the current stress changes onto each major fault, the probability calculations were performed and given for the whole study area during the next 30 years.

Key words: *Greece, strong earthquakes, coseismic stress changes, stress transfer, earthquake probabilities, seismic hazard.*

1. Introduction

Many destructive earthquakes occurred in the territory of Greece and the adjacent areas, some of them being close both in time and space. For this reason the investigation of possible connection of these occurrences through stress transfer is of paramount importance for seismic hazard purposes. Thus, the first goal of the present study is to calculate the coseismic stress changes caused by the strong earthquakes of $M \geq 6.5$ that occurred during the instrumental era that is since the beginning of the 20th century in the study area. As a second step the static stress changes on specific faults that have accumulated until now will be incorporated into probabilistic models, in an attempt to assess the seismic hazard in the study area.

Earthquake triggering or delay due to changes in stress was recognized more than a decade ago (e.g.

Harris, 1998 and references therein) and is worked out in assessing earthquake occurrence and future seismic hazard in a certain area. Stein (1999), reviewing the role of stress transfer, emphasized the earthquake interaction as a fundamental feature of seismicity, that promises a deeper understanding of the earthquake occurrence and a better description of the seismic hazard, when stress transfer is incorporated into probability models (Stein et al., 1997; Toda et al., 1998). In association with physical fault models and fault properties, such models were more developed and statistically assessed (Parsons, 2004, 2005 among others). Another investigation, in the area of Western Turkey, was performed by Paradisopoulou et al. (2010) who calculate static stress changes of $M \geq 6.5$ events and estimated the probability of an earthquake occurrence in the next 30 years from 2008.

The present study differs from the previously mentioned ones in calculations of static stress changes and estimation of probabilities for the whole territory of Greece and its adjacent areas. We start with the stationary and conditional probability models estimating the probability of occurrence in the next 30 years from the studied date (2009) of an earthquake with $M \geq 6.5$ on known fault segments of the study area. Then the accumulated stress changes due to coseismic slips of the modeled events are incorporated into the estimation of earthquake probability. Change in the probability on a given fault is calculated from the change in seismicity rate, which is computed by taking into account both permanent and transient effects.

2. Stress change calculations

The Coulomb stress changes are calculated for earthquakes with $M \geq 6.5$ that occurred in the study area since 1900. An earthquake can be modelled as a slipping dislocation in an elastic half space (Okada, 1992) enabling estimation of stress transfer to other faults. Earthquakes occur when stress exceeds the strength of the fault. The closeness to the failure is quantified using the change in Coulomb failure function (ΔCFF). In its simplest form, the Coulomb failure stress change is (modified from Scholz, 1990) (eq. 1):

(1)

where $\Delta\tau$ is the change in shear stress on a fault (set positive in the direction of fault slip), $\Delta\sigma$ is the change in normal stress (set positive for extension) and μ' is the apparent coefficient of friction, which is assumed to incorporate changes in pore pressure (Harris and Simpson 1998) and material properties of the fault zone. $\Delta\sigma$ and $\Delta\tau$ are calculated for a fault plane at the observing (field) point. For increasing shear stress in the direction of relative slip on the observing fault $\Delta\tau$ is positive. $\Delta\sigma$ is positive for tensional normal stress. The shear modulus and Poisson's ratio are fixed at $3.3 \cdot 10^5$ bar and 0.25, respectively. Coulomb stress changes are calculated according to the geometry of the target fault, which is the fault of the subsequent strong earthquake in our sample, and at the appropriate depth. In our study area it is known that the majority of the foci of the crustal earthquakes are located in the depth range of 3 to 15 km, which defines the brittle part of the crust. Considering all the above information the seismogenic layer in our calculations is taken to be in this range for all the strong events ($M \geq 6.5$) modeled, and stress changes are calculated at the depth of 10km.

3. Probability Calculations

3.1 Methodology

An attempt is made in this section to estimate probabilities for the occurrence of future strong ($M \geq 6.5$) events on the fault segments associated with events of $M \geq 6.5$ that occurred either during the instrumental period or in the past centuries and for which available information exists. For a

probabilistic earthquake forecast in a region under the influence of past events it is considered that the stress transfer might fasten or delay the next earthquake. The methodology followed is that by Stein et al. (1997); Toda et al. (1998) and Parsons (2004, 2005) who considered both permanent and transient effect of the stress changes on earthquake probabilities.

Two models for estimation of earthquake probabilities are generally in use: the stationary Poisson model and the conditional probability model (Cornell et al., 1968; Hagiwara, 1974). Using both of the mentioned models we estimate the probability of an earthquake to occur in the next 30 years from 2009.

- Poisson model: This model is one that treats earthquakes as occurring at random in time (t) about an average interevent time (T_p). The probability of at least one event in the time interval ($t, t+\Delta t$) is given by:

(2)

- Conditional Probability model: In this model, probability can increase with time to represent increasing stress on a fault segment toward an uncertain stress threshold. A time-dependent probability (in any time interval ($t, t+\Delta t$)) is calculated by a probability density function $f(t)$ as (Working Group of California Earthquake Probabilities, 1990):

(3)

where P is the probability that an earthquake will recur at some time T in the interval ($t, t+\Delta t$) and $f(t)$ is the applied probability density function of recurrence time. The probability, conditional on the earthquake not occurring prior to t , is:

(4)

We assume a lognormal probability distribution of recurrence time (e.g. Nishenko and Buland, 1987):

(5)

where \bar{T} is the average interevent time, s_t : the standard deviation of interevent time.

- Permanent effect of stress change: Increasing (or decreasing) Coulomb stress on a fault segment permanently shortens (or lengthens) the time required for tectonic stressing to bring the segment to failure and thus causes a permanent change in conditional probability. The conditional probability model can be adapted to estimate the effect of stress changes by equating the stress change with the time required to accumulate stress through secular stressing. Therefore, for the calculation of the probability for the fault of interest an adjusted time by the clock change must be taken into account. The 'life clock change' of the fault of interest can be estimated by:

(6)

where ΔCFF : is the stress change due to nearby event and $\dot{\sigma}$ is the tectonic stressing rate in bar/yr. Thus, to calculate the conditional probability for the fault of interest taking into account an adjusted time by the clock change the following equation is used:

(7)

- Transient effect of stress change: The existence of foreshocks and aftershocks demonstrate that when an earthquake occurs there is a large transient increase in the probability of additional earthquakes in the surrounding area. A quantitative explanation of aftershock distributions and decay, and foreshock statistics, is given by a single model in which the rate of earthquake occurrence is perturbed by the local stress changes caused by a prior earthquake (Dieterich, 1994; Dieterich & Kilgore, 1996). We use this model to estimate the rate–state transient effect that describes an expected enhanced rate of earthquake nucleation resulting from a stress increase and can be expressed as a probability. For a stress decrease the rate of nucleation declines and eventually recovers. Because the transient effect of the stress change is expressed as a change in expected rate of segment events, it is convenient to formulate the probability analysis as a non–stationary Poisson process in which the probability of an earthquake occurring in the interval $(t, t+\Delta t)$ is given by:

(8)

where, P is the net probability, which combines the transient and permanent effects of the stress change on earthquake probability and $R(t)$ is the expected earthquake rate following a stress step. Δt is measured from the time of the stress step (we use 30 years for these computations). To evaluate eq. (2), we obtain N , by integrating the solution for $R(t)$ following a stress step (Dieterich, 1994). For the interval 0 to Δt , this yields:

(9)

where r_p is the permanent background component of the earthquake rate following the stress step:

(10)

where P_c is the permanent probability from eq. 7, t_α is the characteristic duration of the transient effect, σ , is the normal stress, A , is a fault constitutive constant and ΔCFF is the calculated Coulomb stress change. Note that the transient effect disappears if $\Delta CFF=0$, that is $N=r_p \cdot \Delta t$. We calculated $A\sigma$ of eq. (9) by knowing the parameters t_α and ΔCFF and using the equation (Dieterich, 1994):

(11)

3.2 Parameter calculations

- Mean interevent time (T_r): For this estimation it was necessary to collect historical information and paleoseismological investigations for earthquakes with $M \geq 6.5$ that associated with fault segments of the study area. Historical information are mainly taken from Papazachos and Papazachou (2003), Ambraseys and Jackson (2000) and Ambraseys (2002). Some of paleoseismic records are found on the North Anatolian Fault (NAF). This information is useful especially in the cases of large events that seem to have broken multiple segments or in cases of clustering, like the three large earthquakes in 1343, 1344 and 1354, which according to Rockwell et al. (2001), comprise a mini-sequence rupturing much of the NAF. At Duzce fault (S127) there are 3 events observed (Pantosti et al., 2008), 2 events are noted at nearby Izmit segment (S125) (Parsons, 2004; Pondard et al. 2007; Klinger et al. 2003) and 3 events are associated with the Cinarcik (S124) segment, with an observed mean frequency of 170 years and a modelled ~ 250 year interevent time (Parsons, 2004; Pondard et al. 2007). At Marmaras 1 and 2 (S123, S122 respectively) 3 and 4 events observed according to Parsons (2004) and Papazachos and Papazachou (2003). Observations on the Ganos fault (S121) support $T_r \sim 275$ years (Rockwell et al., 2001). Parsons (2004) gives a calculated mean interevent time of 207 years. Paleoseismological data for Mudurnu segment and Yenice fault are taken from Palyvos et al. (2007) and Kurcer et al. (2008).

In the area of Corinth Gulf, in Eliki's (S43) and Xylokaastro fault (S44), a mean interevent time of 242 ± 60 years and 119 ± 20 years was found respectively (Briole et al., 2000). The Eliki fault is associated with 373 B.C. and 1748, 1861 earthquakes result an average time 270-1200 years (Koukouvelas et al. 2001). Collier et al. (1998) give a calculated mean interevent time equal to 330 years. According to Pavlides et al. (2004) one paleoearthquake occurred before 1894 earthquake on Atalanti's fault supporting a mean interevent time of 1000 years. Pantosti et al. (2004) are estimated, for the same fault, a mean interevent time of 660-1200 years.

Using all the above data the mean interevent time (T_r) is calculated for each segment of the study area. In cases where only one or two events were reported for a particular fault segment, the interevent times are set equal to 500 years. Table 1 gives the calculated values of T_r for some faults of the study area.

- Duration of transient effect (t_a): Dieterich (1994) based on the constitutive formulation for rate of earthquake activity, derived from laboratory observations of rate- and state-dependent fault properties. A consequence of clustering statistics and time-dependent nucleation is that earthquake rates at all magnitudes undergo a strong transient amplification at the time of a step increase of stress, followed by $1/t$ decay to their background rate. In the present study, t_a was set equal to 10% of the minimum interevent time. Thus, for the area of North Anatolian fault $t_a = 25$ yr, considering a minimum return period of 250 years. For the same area a regional aftershock decay time for $M \geq 6.7$ earthquakes was found to be ~ 35 years by Parsons et al. (2000). A value of $t_a = 50$ yr was set for the rest part of our study area due to the longer observed interevent times (~ 500 years). For the southern part of Corinth Gulf the t_a was set equal to 30 years and for the Ionian Sea equal to 10 years because at these areas the mean interevent times are smaller.
- Tectonic stressing rate ($\dot{\sigma}$): This parameter is important for the calculation of T' (eq. 6) and consequently the permanent probability P_c (eq. 7). Stressing rates are calculated in each fault segment from the yearly slip rate. For parts of North Anatolian Fault, $\dot{\sigma}$ is found equal to 0.04-0.25 bar/yr with a mean value 0.10 bar/yr. These values are in agreement with the ones from Stein et al. (1997), who estimated a value of 0.15 bar/yr along most of the NAF system and from Parsons et al. (2000) who

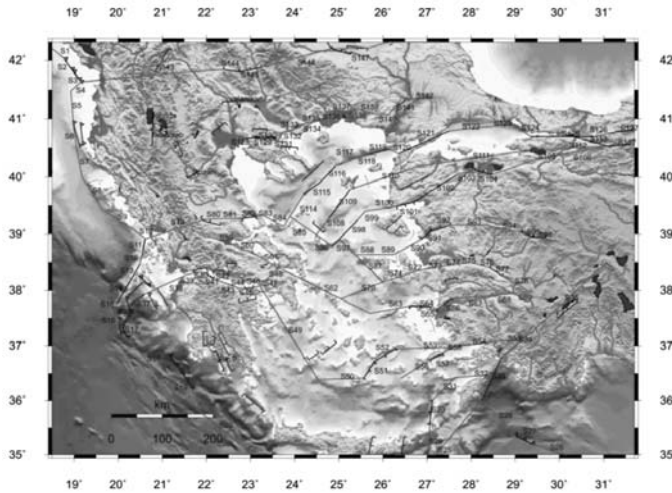


Fig. 1: Map of the main active structures of the study area (red color) along with the faults for which the coseismic changes were calculated (black colors). The faults that are associated with historical earthquakes of $M \geq 6.5$ are shown in blue. The code names of fault segments are shown next to each segment.

calculated $\dot{\sigma} = 0.1 \text{ bar/yr}$, and Parsons (2004) with values of $\dot{\sigma}$ in the range of $0.01\text{-}0.064 \text{ bar/yr}$. For the remaining part of the study area the values of stressing rate are in the range of $0.003\text{-}0.25 \text{ bar/yr}$.

- **Coulomb Stress Changes (ΔCFF):** The ΔCFF value on each fault segment is achieved by extending the calculations of the accumulated static stress changes due to the coseismic slip of the modeled events up to 2009. Since uncertainties are involved in these estimations and because stress change is spatially variable, we consider three different values, i.e, the minimum, maximum and average calculated ΔCFF values, and consequently three different clock changes values as revealed from eq.6 and three values of permanent probability (eq. 7). The effect of the stress step in the probability estimates becomes more evident in the cases where the fault segment has recently failed (e.g Izmit, Duzce and Methoni faults) and where a fault segment is located along strike with a previously failed segment, resulting in the positive static stress changes on the first segments. In these cases the differences between the probability estimates before and after the stress step are significant and must be included in any assessment for the future seismic hazard.
- **Probability calculations:** We first calculate the probability using Poisson model (eq. 2) and Conditional probability model (eq. 4) using $\Delta t = 30 \text{ years}$ for all fault segments of the study area (S1-S148) and for some individual faults that are connected with historical strong ($M \geq 6.5$) events (fig. 1). The net probability (eq. 8) of events rupturing each fault segment combines both the permanent and transient effects of a stress step. Net probability is obtained first by computing the permanent effect of a stress change on the conditional probability using eq. (7). Then the equivalent background rate r_p for the permanent effect is obtained using eq. (10) to evaluate eq. (9) and eq. (8) for the net probability.

4. Results and Conclusions

The present study is an effort to interpret the occurrences of strong ($M \geq 6.5$) earthquakes in Greece and broader area and to evaluate the future seismic hazard incorporating Coulomb Stress changes (ΔCFF) to probability estimates. Generally different parameters, such as the duration of transient effect (t_a), the stressing rate $\dot{\sigma}$ and stress step (ΔCFF), were taken into account for probability calculations. The affect of the stress step becomes more evident in the cases in which the fault segment has

Table 1. Estimated 30 year probabilities larger than 0.10. The first column is the code name of each fault segment. The second column gives the recurrence time, T_r , and the third column gives the stressing rate of each segment in bars/yr. The fourth and fifth columns give the Poissonian and Conditional probabilities. The three next columns give the minimum, maximum and average probability of occurrence for the next 30 years modified by the permanent effect of ΔCFF . The last three columns give the corresponding probabilities modified by both the permanent and transient effect of ΔCFF .

Segment Code Name	Tr (years)	Stressing Rate $\dot{\tau}$ (bars/year)	Cond. probability before the stress step		Cond. probability after the stress step (Permanent effect)			Cond. probability after the stress step (Permanent + Transient effect)		
			Poison	Conditional	Min P(30)	Max P(30)	Avg P(30)	Min P(30)	Max P(30)	Avg P(30)
S11	82.5	0.0817	0.3049	0.4995	0.3074	0.4876	0.3745	0.2583	0.4843	0.3404
S13	85.7	0.1756	0.2954	0.6963	0.0031	0.9293	0.4172	0.0001	0.9505	0.3660
S20	124	0.0073	0.2149	0.4215	0.0000	1.0000	0.3953	0.0000	0.9997	0.3956
S22	500	0.0198	0.0582	0.1171	0.0001	0.7494	0.1329	0.0000	0.7789	0.1338
S43	113	0.0522	0.2332	0.4496	0.4410	0.5638	0.4773	0.4407	0.5663	0.4782
S44	145	0.0445	0.1869	0.2567	0.2499	0.2929	0.2617	0.2500	0.2922	0.2617
S67	246	0.0425	0.1148	0.1041	0.1000	0.2992	0.1123	0.0956	0.5282	0.1214
S69	500	0.0529	0.0582	0.0923	0.0931	0.0935	0.0934	0.0932	0.0938	0.0936
S100	137	0.0275	0.1967	0.3908	0.3878	0.9878	0.6311	0.3877	0.9778	0.6300
S103	1013	0.0197	0.0292	0.0218	0.1454	0.9472	0.3646	0.2530	0.9990	0.7162
S122	141	0.2583	0.1917	0.3815	0.3689	0.3733	0.3721	0.3691	0.3734	0.3722
S123	298	0.2041	0.0958	0.1979	0.0013	0.2989	0.1848	0.0009	0.3024	0.1844
S124	281	0.2147	0.1013	0.0756	0.0808	0.3347	0.1174	0.0850	0.6589	0.1597
Edessa	500	0.0075	0.0582	0.1236	0.1317	0.1414	0.1381	0.1319	0.1418	0.1385
Tetovo	500	0.0067	0.0582	0.1146	0.1279	0.1493	0.1384	0.1277	0.1487	0.1380
Eratini	399	0.0254	0.0724	0.0830	0.0254	0.0883	0.7489	0.2058	0.0909	0.9334
Messini	500	0.0076	0.0582	0.0217	0.0365	0.1394	0.0623	0.0631	0.5031	0.1625
Kalamata	500	0.0093	0.0582	0.0946	0.0093	0.1803	0.2570	0.2089	0.1989	0.2957

recently failed (e.g. Izmit segment, S125) and where a fault segment is located along strike with previously failed segment, resulting in the positive static stress changes on the first segments. In these cases different probability values were estimated before and after the stress step and these differences must be included in any assessment for the future seismic hazard. Moreover, the choice of tectonic stressing rate has a significant effect to the final probability results. The $\dot{\tau}$ is related with the time, T_r , and therefore it could be for example lead to smaller clock changes for a given stress change, and hence to smaller probability values. For this reason several values of $\dot{\tau}$ have been used for each fault zone as already mentioned. The duration of the transient effect (t_q) has been used to calculate both

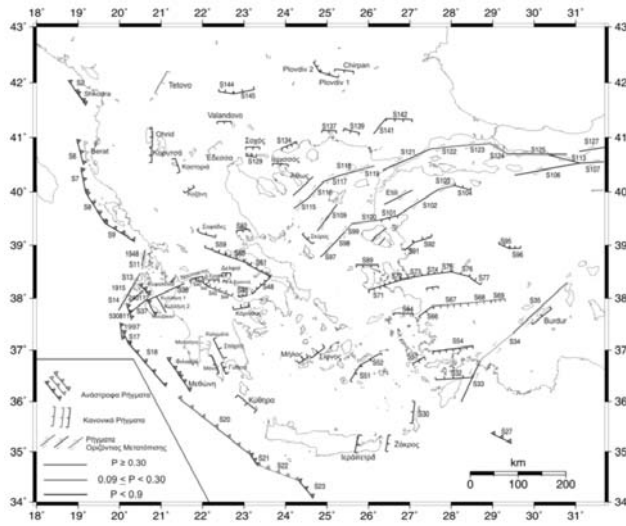


Fig. 2: Map of estimated time dependent probabilities for the occurrence of an earthquake with magnitude $M \geq 6.5$ for next 30 years (after 2009), in each fault segment of the study area. The values of probability and the corresponding color are depicted in the inset at the lower left corner of the map.

the $A\sigma$ factor and the net probability. For this calculation we were based on Dieterich (1994) and t_{α} was set $\sim 10\%$ of mean interevent time (T_p) for each fault segment. The detailed value of t_{α} for each area affect our results but this estimation cannot be analysed in the framework of this study.

In more detail, probability estimations are carried out for 148 fault segments (S1-S148) and for faults that are related with historical earthquakes of $M \geq 6.5$. Calculations are not performed for the fault segments where there is not information available for the occurrence of such events. Due to the large amounts of data the calculated parameters needed to estimate probabilities and the values of estimated time dependent probabilities are given in Table 1 only for some faults of the study area for which the value of the net, average, probability is considered greater than 0.10.

Fig. 2 shows the fault segments for which the time dependent probability is estimated for the occurrence of an earthquake with $M \geq 6.5$ for next 30 years after the studied date (2009). The color of each fault corresponds to the mean value of estimated probabilities after permanent and transient effect. For low probability values ($P < 0.09$) the fault has blue color while green and red color indicate higher probability values ($0.09 \leq P < 0.30$ and $P \geq 0.30$, respectively).

The first result in probability estimates is that for some of the segments the values that have been calculated from the renewal model based on the lognormal distribution are different from those values based on the Poisson model ranging between 5% and 35%. These results are in agreement with previous investigations, especially at Marmara and Izmit region (Stein et al., 1997; Parsons, 2004). The variation between the values occur due to the following reasons: For the conditional probabilities estimations, we use mean interevent time equal to 500 years for some fault segments, because reliable historical information was not available. In the cases where the Poissonian probabilities are larger than the conditional ones for some fault segments, the time elapsed since the last event of $M \geq 6.5$, is shorter than the estimated mean interevent time. In addition, for the same mean interevent time, the Poissonian probability model estimation, that treats earthquakes as occurring at random in time, is different from conditional probabilities model which takes into account the time passed from the last earthquake in a fault. Therefore, we consider that the results from time dependent probability estimation are more reliable than the Poissonian ones. Generally the uncertainties involved in

these estimates concern the mean interevent time and the corresponding standard deviation, the aftershock duration (t_a) and the value of $A\sigma$ (we calculate the $A\sigma$ value using eq. (11) considering that t_a is known from previous investigations).

The ΔCFF values, calculated according to the faulting type of each fault segment, are incorporated into the probability estimates, as the permanent stress effects and both the permanent and transient effects. For this purpose we consider minimum, maximum and average values of ΔCFF , as well as the minimum, maximum and average values of clock advance or delay (eq. 6). It is interesting to note that these values affect the estimated probabilities, by increasing them in comparison with Poissonian and increasing the conditional probability estimates when positive values of ΔCFF are found on the certain fault segment, or decreasing them in the cases of negative corresponding ΔCFF values. For example, in the Izmit fault segment, the ΔCFF effect decreases substantially the conditional probabilities (by a factor of 10^{-5}). The stress transfer between adjacent fault segments considerably influences the probability estimates. For certain fault segments the differences between Poissonian and conditional estimates before the stress step are significantly different than the ones incorporating the stress step, and worth to be mentioned for the future seismic hazard assessment. For example, for the fault segments along the north Marmara Sea (S122, S123 and S124) the Poissonian probabilities found equal to 0.19, 0.09 and 0.10, respectively, whereas the corresponding time dependent ones equal to 0.38, 0.18 and 0.16, respectively.

The opposite but also significant consequence of ΔCFF effect is observed for the Izmit (S125) and Duzce (S127) segments last ruptured in 1999, yielding a 30-year Poisson probability of 0.10 and 0.05, respectively, whereas the time-dependent probabilities on these segments are $\sim 0\%$. The calculated probability value for the area of North Aegean Sea found equal to 0.63 for Edremit fault segment (S100) and 0.7 in north western Turkey (Yenise, S103). In the area of Ionian Sea the Lefkada (S11) and Kefalonia (S13) fault segments ruptured in 1940-1960 indicating low mean interevent times. The time dependent probability estimated 0.34 and 0.36 for S11 and S13 faults respectively. The ΔCFF effect resulted in high probability estimates for normal fault segments being along strike with previous ruptures, in the study area. Specifically for Aydin (S67) and Denizli (S69) fault segments in central western Turkey the mean probability value after permanent and transient effect is estimated 0.12 and 0.10 respectively whereas in the area of Corinth Gulf the calculated time dependent probabilities were 0.47 and 0.26 for the Eliko (S43) and Xylokstro (S44) fault segments, respectively. For fault segments with N-S direction such as Tetovo fault in the northern of the study area and in south Messini fault (Peloponnesus) the corresponding probabilities are equal to 0.13 and 0.16, respectively. For Edessa and Kalamata faults the probability estimated 0.23 and 0.14 respectively. These values are high for this area because two strong earthquakes occurred (1986, $M=6.0$, in Kalamata and 1990 $M=6.0$ in Edessa) but both of them are under 6.5 so we do not take them into account. The results from probability estimates for reverse faults indicate high values in Tenaro (S20) (0.40) and Elafonisos (S22) (0.13) fault segments respectively.

5. Acknowledgments

The stress tensors were calculated using a program written by J. Deng (Deng and Sykes, 1997) based on the DIS3D code of S. Dunbar, which later improved (Erikson, 1986) and the expressions of G. Converse. The GMT system (Wessel and Smith, 1998) was used to plot the figures. This work was partially supported by the research project No. 11.11.140.767, financed by the Polish State Committee for Scientific Research, AGH University of Science and Technology, Faculty of Geology, Geophysics and Environmental Protection. Geophysics Department contribution 757.

6. References

- Ambraseys, N. N., 2002. The seismic activity of the Marmara Sea region over the last 2000 years. *Bulletin Seismological Society of America* 92, 1-18.
- Ambraseys, N. N., and J. A. Jackson, 2000. Seismicity of Marmara (Turkey) since 1500. *Geophysical Journal International* 141, F1-F6.
- Briole, P., Rigo, A., Lyon-Caen, H., Ruegg, J.C., Papazissi, K., Mitsakaki, C., Balodimou, A., Veis, G., Hatzfeld, D. and Deschamps, A., 2000. Active deformation of the Corinth rift, Greece: Results from repeated Global Positioning System surveys between 1990 and 1995. *Journal of Geophysical Research* 105, 605-625.
- Chatzipetros, S., Kokkalas, S., Pavlides, S., and Koukouvelas, I., 2005. Palaeoseismic data and their implication for active deformation in Greece, *Journal of Geodynamics*, 40, 170-188A.
- Collier, R. E., Pantosti, D., D'addezio, G., De Martini, P.M., Masana, E. and Sakellariou, D., 1998. Palaeoseismicity of the 1981 Corinth earthquake fault: seismic contribution to extensional strain in central Greece and implications for seismic hazard. *Journal of Geophysical Research* 103, 30001-30019.
- Cornell, C. A., Wu, S. C., Winterstein, S. R., Dieterich, J. H. and Simpson, R. W., 1968. Seismic hazard induced by mechanically interactive fault segments. *Bulletin Seismological Society of America* 83, 436-449.
- Deng, J. and Sykes, L., 1997. Evolution of the stress field in Southern California and triggering of moderate size earthquakes: A 200-year perspective. *Journal of Geophysical Research* 102, 9859-9886.
- Dieterich, J. H., 1994. A constitutive law for rate of earthquake production and its application to earthquake clustering. *Journal of Geophysical Research* 99, 2601-2618.
- Dieterich, J. H. and Kilgore, B., 1996. Implications of fault constitutive properties for earthquake prediction. *Proceedings of the National Academy of Sciences U.S.A*, 93, 3787-3794.
- Erikson, L., 1986. User's manual for DIS3D: A three-dimensional dislocation program with applications to faulting in the Earth. Master's Thesis, Stanford Univ., Stanford, Calif., pp. 167.
- Hagiwara, Y., 1974. Probability of earthquake occurrence as obtained from a Weibull distribution analysis of crustal strain, *Tectonophysics*, 23, 313-318.
- Harris, R. A., 1998. Introduction to special section: Stress triggers, stress shadows and implications for seismic hazard. *Journal of Geophysical Research* 103, 24,347-24,358.
- Harris, R. and Simpson, R., 1998. Suppression of Large Earthquakes by Stress Shadows: A Comparison of Coulomb and Rate – and – State Failure. *Journal of Geophysical Research* 103, 24439-24451.
- Hubert-Ferrari, A., Barka, A., Jacques, E., Nalbat, S.S., Meyer, B., Armijo, R., Tapponnier, P. and King, C. P. G., 2000. Seismic hazard in the Sea of Marmara following the 17 August 1999 earthquake. *Nature* 404, 269-272.
- Klinger, Y., Sieh, K., Altunel, E., Akoglu, A., Barka, A., Dawson, T., Gonzalez, T., Meltzner, A. and Rockwell, T., 2003. Paleoseismic Evidence of Characteristic Slip on the Western Segment of the North Anatolian Fault, Turkey. *Bulletin of Seismological Society of America* 93, 2317-2332.
- Koukouvelas, I.K., Stamatopoulos, L., Katsanopoulou, D. and Pavlides, S., 2001. A palaeoseismological and geoarchaeological investigation of the Eliki fault, Gulf of Corinth, Greece. *Journal of Structural Geology* 23, 531-543.
- Kurcer, A., Chatzipetros, A., Tutkun, S. Z., Pavlides, S., Ates, O. and Valkaniotis, S., 2008. The Yenice-Gonen active fault (NW Turkey): Active tectonics and palaeoseismology. *Tectonophysics*, 453, 263-275.
- Nishenko, S. P. and Buland R., 1987. A generic recurrence interval distribution for earthquake forecasting. *Bulletin Seismological Society of America* 77, 1382-1399.
- Okada, Y., 1992. Internal deformation due to shear and tensile faults in a half space. *Bulletin of Seismo-*

logical Society of America 82, 1018-1040.

- Palyvos, N., Pantosti, D., Zabcı, C. and D' Addezio, G. 2007. Paleoseismological evidence of recent earthquakes on the 1967 Mudurnu valley earthquake segment of the North Anatolian Fault zone. *Bulletin Seismological Society of America* 97, 1646–1661.
- Pantosti, D., De Martini, P.M., Papanastassiou, D., Lemeille, F., Palyvos, N. and Stavrakakis, G. 2004. Paleoseismological Trenching across the Atalanti Fault (Central Greece): Evidence for the Ancestors of the 1894. Earthquake during the Middle Age and Roman Times. *Bulletin Seismological Society of America* 94, 2, 531-549.
- Pantosti, D., Pucci, S., Palyvos, N., De Martini, P. M., D' Addezio, G., Collins, P. E. F. and Zabcı, C., 2008. Paleoequakes of the Düzce fault (North Anatolian Fault Zone): Insights for large surface faulting earthquake recurrence. *Journal of Geophysical Research* 113, doi:10.1029/2006JB004679.
- Papazachos, B. C. and Papazachou, C., 2003. *The earthquakes of Greece*. Ziti publications, Thessaloniki, pp. 289.
- Paradisopoulou, P. M., Papadimitriou, E. E., Karakostas, V. G., Taymaz, T., Kilas, A., and Yolsal, S., (2010). Seismic hazard evaluation in western Turkey as revealed by stress transfer and time-dependent probability calculations. *Pure and Applied Geophysics* doi: 10.1007/s00024-010-0085-1.
- Parsons, T., 2004. Recalculated probability of $M \geq 7$ earthquakes beneath the Sea of Marmara, Turkey. *Journal of Geophysical Research* 109, doi:10.1029/2003JB002667.
- Parsons, T., 2005. Significance of stress transfer in time-dependent earthquake probability calculations. *Journal of Geophysical Research* 110, doi: 10.1029/2004JB003190.
- Parsons, T., Toda, S., Stein, R. S., Barka, A. and Dieterich, J. H. (2000). Heightened odds of large earthquakes near Istanbul: An interaction-based probability calculation, *Science*, 288, 661–665.
- Pavlıdes S.B., Valkaniotis S., Ganas A., Keramydas D. and Sboras S., 2004. The Atalanti active fault: re-evaluation using new geological data. Bulletin of the Geological Society of Greece vol. XXXVI, *Proceedings of the 10th International Congress*, Thessaloniki, 1560-1567
- Pondard, N., Armijo, R., King, G. C. P., Meyer, B. and Flerit, F., 2007. Fault interactions in the Sea of Marmara pull-apart (North Anatolian Fault): earthquake clustering and propagating earthquake sequences. *Geophysical Journal International* 171, 1185–1197.
- Rockwell, T., Barka, A., Dawson, T., Akyuz, S. and Thorup, K., 2001. Paleoseismology of the Gazikoy–Saros segment of the North Anatolia fault, northwestern Turkey: Comparison of the historical and paleoseismic records, implications of regional seismic hazard and models of earthquake recurrence. *Journal of Seismology* 5, 433–448.
- Scholz, C., 1990. *The mechanics of earthquakes and faulting*. Cambridge University Press, Cambridge, pp. 439.
- Stein, R. S., 1999. The role of stress transfer in earthquake occurrence. *Nature* 402, 605-609.
- Stein, R.S., Barka, A.A., and Dieterich, J.D., 1997. Progressive failure on the North Anatolian fault since 1939 by earthquake stress triggering. *Geophysical Journal International* 128, 594-604.
- Toda, S., Stein, R. S., Reasenberg, P. A., and Yoshida, A., 1998. Stress transferred by the 1995 Mw=6.9 Kobe, Japan shock: Effect on aftershocks and future earthquake probabilities. *Journal of Geophysical Research* 124, 439-451.
- Wessel, P., and Smith, W. H. F., 1998. New improved version of the Generic Mapping Tools Released. *EOS Trans. AGU* 79, 579.
- Working Group on California Earthquake Probabilities (WGCEP), 1990. Probabilities of large earthquakes in the San Francisco Bay region. California, *U.S. Geol. Surv. Circ.* 1053, 51.